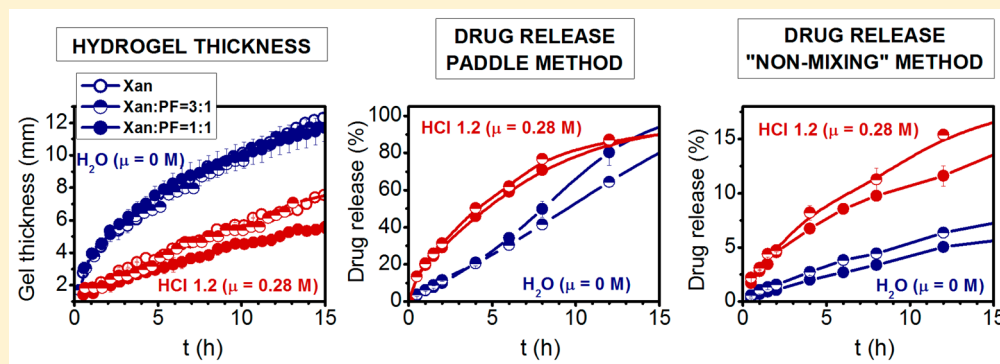


# The Influence of High Drug Loading in Xanthan Tablets and Media with Different Physiological pH and Ionic Strength on Swelling and Release

Urša Mikac,<sup>\*,†</sup> Ana Sepe,<sup>†</sup> Saša Baumgartner,<sup>‡</sup> and Julijana Kristl<sup>‡</sup>

<sup>†</sup>Jožef Stefan Institute, 1000 Ljubljana, Slovenia

<sup>‡</sup>Faculty of Pharmacy, University of Ljubljana, 1000 Ljubljana, Slovenia



**ABSTRACT:** The formation of a gel coat around xanthan (Xan) tablets, empty or loaded with pentoxifylline (PF), and its release in media differing in pH and ionic strength by NMR, MR imaging, and two release methods were studied. The  $T_1$  and  $T_2$  NMR relaxation times in gels depend predominantly on Xan concentration; the presence of PF has negligible influence on them. It is interesting that the matrix swelling is primarily regulated by Xan despite high drug loading (25%, 50%). The gastric pH and high ionic strength of the media do not influence the position of the penetration and swelling fronts but do affect the erosion front and gel thickness. The different release profiles obtained in mixing and nonmixing *in vitro* methods are the consequence of matrix hydration level and erosion at the surface. In water and in diluted acid medium with low ionic strength, the main release mechanism is erosion, whereas in other media (pH 1.2,  $\mu \geq 0.20$  M), anomalous transport dominates as was found out by fitting of measured data with theoretical model. Besides the *in vitro* investigation that mimics gastric conditions, mathematical modeling makes the product development more successful.

**KEYWORDS:** oral drug formulations, matrix tablets, gel thickness, magnetic resonance imaging, drug release mechanisms, mathematical modeling, pH-controlled release

## 1. INTRODUCTION

Hydrophilic matrix tablets have been commonly used for many years to provide sustained drug delivery. Upon contact of the matrix tablet with body fluids, polymer chains hydrate and swell, forming a gel coat around the tablet that regulates further penetration of fluids. For successful drug release, the drug must first transform from an undissolved state into a dissolved state, and it may afterward diffuse through the gel layer.<sup>1,2</sup> Numerous experienced research groups have reported that, despite the well-known mechanisms of gel formation around the dry matrix core and drug release kinetics *in vitro*, there is a significant inherent obstacle to the success of clinical or bioequivalent studies for developing new therapeutic products. Because the physiological parameters change progressively in the gastrointestinal tract,<sup>3</sup> it is important to understand the swelling behavior of matrix tablets under different pH and ionic strengths of gastric fluids as well as their impact on incorporated drug. The fact is that in matrix tablets a number of processes are taking place at the same time and usually these

processes have been investigated individually, independently from one another, and using different methods.<sup>4–6</sup> Therefore, there is a lot of specific information but rather few comprehensive reports and conclusions.

The polymer matrix swelling process has been studied using a variety of techniques such as rheology, thermal analysis, optical rotation, light scattering, size exclusion chromatography, optical imaging, ultrasound, and texture analysis, and later NMR and magnetic resonance imaging (MRI) as well.<sup>7–16</sup> To be able to measure polymer swelling and drug release simultaneously and under the same experimental conditions, a combination of MRI and the USP-4 apparatus has been developed.<sup>17,18</sup> The same advantage was achieved by volume-localized magnetic resonance spectroscopy<sup>19</sup> and chemical shift

**Received:** December 17, 2015

**Revised:** February 5, 2016

**Accepted:** February 11, 2016

**Published:** February 11, 2016

imaging.<sup>20</sup> With <sup>1</sup>H and <sup>19</sup>F MRI, gel thickness and drug concentration in the gel layer as well as in the surrounding medium have been determined simultaneously.<sup>21–23</sup>

The dominant matrix excipients for the majority of modified-release formulations are hydrophilic polymers that can be of semisynthetic or natural origin. Among them, hydroxypropyl methylcellulose is the most frequently studied,<sup>2,7–9,11,13,21,24</sup> while xanthan (Xan) produced biotechnologically by the bacterium *Xanthomonas campestris* is also a well-known and already widely used biopolymer.<sup>25</sup> Chemically, Xan is a heteropolysaccharide consisting of a β,1–4-D-glucose backbone. The presence of glucuronic acid as well as pyruvate acid groups is mainly responsible for its anionic polyelectrolyte character. It is used in controlled drug delivery formulations and in the food and cosmetics industry as a thickening agent or a stabilizer mostly associated with the modification of viscosity due to swelling. The native ordered and rigid conformation of Xan chains has been reported to exist as a double-strand helix,<sup>26</sup> although a single helical conformation has also been proposed.<sup>27</sup> In solution, the rigid helix–coil structure transforms into flexible coils. This polymer is a weak acid (pK<sub>a</sub> 3.1) that exhibits pH-dependent swelling and solubility. The changes in Xan swelling and solubility at different pH may cause changes of dissolution profiles and the reduction of drug release and efficacy. In fact, *in vitro* dissolution methodologies that assess the impact of physiological changes in the GI condition are expected to better predict *in vivo* dissolution of oral delivery systems and, hence, better assess efficacy, toxicity, and safety concerns. The major goals of *in vitro* dissolution are to ensure the performance of oral drug products and the support of drug formulation design.<sup>28</sup>

The objective of the present study is to determine the changes in xanthan tablets with high drug loading after contact with various physiological media to predict *in vivo* swelling and drug release. The specific aim was to study: (i) the effect of high drug loading on  $T_1$  and  $T_2$  relaxation times of xanthan gels, (ii) the effect of drug loading on swelling and erosion behavior of xanthan tablets in various media, (iii) the influence of *in vitro* dissolution conditions (rotating and “non-mixing” method) on drug release and release kinetics, (iv) as realistic as possible interpretation of the influence of high drug loading on xanthan gel layer properties and drug release comparing experimental results and theoretical predictions of polymer swelling and drug release.

To test these, we studied Xan tablet swelling in various media and the influence of pentoxifylline (PF), a highly soluble, nonionogenic, model drug, using MRI approaches. The results of PF release from Xan tablets under two different conditions, that is, using a standard paddle method (USP IV model) and static “non-mixing” conditions, in which medium penetration was allowed from only one circular surface, were correlated with mathematical analysis.

## 2. THEORETICAL SECTION

Different mathematical models for polymer swelling and drug release from matrix tablets have been proposed.<sup>29–32</sup> One of them is a simple model developed by Narasimhan and Peppas that was used to describe the hydrophilic polymer swelling kinetics and drug release from matrix tablets (slab or disc) in various media.<sup>33</sup> The prevailing picture of the swelling and release behavior of hydrophilic matrix tablets starts with medium penetration, where the polymer concentration gradient is formed. As the medium penetrates into the tablet, a

penetration front that is the border between the dry and the hydrated glassy polymer, moves from the surface toward the tablet center. When the medium amount is high enough, a phase transition of the polymer from the hydrated glassy state into a rubbery state occurs at swelling front position  $R$ , and polymer chain disentanglement begins. The border between the gel layer and the medium is denoted as erosion front  $S$ . Here, the polymer chains gradually relax and further disentangle, which causes matrix erosion. The model considers two moving boundaries:  $R$  as the swelling front and  $S$  as the erosion front and defines the gel layer thickness as  $S - R$ . A steady-state solution to the model equations gives the dependence of the gel layer thickness at time  $t$  as

$$-\frac{S-R}{B} - \frac{A}{B^2} \ln \left[ 1 - \frac{B}{A}(S-R) \right] = t \quad (1)$$

and the expression for the fraction of the released drug  $M_d$  at time  $t$  normalized with respect to the drug released at infinite time ( $M_{d\infty}$ ) as

$$\frac{M_d}{M_{d\infty}} = \frac{v_{deq} + v_d^*}{l} (\sqrt{2At} + Bt) \quad (2)$$

Here,  $A$  and  $B$  are given as

$$A = D_1(v_{1eq} - v_1^*) \left( \frac{v_{1eq}}{v_{1eq} + v_{deq}} + \frac{1}{v_1^* + v_d^*} \right) + D_d(v_d^* - v_{deq}) \left( \frac{v_{deq}}{v_{1eq} + v_{deq}} + \frac{1}{v_1^* + v_d^*} \right) \quad (3)$$

and

$$B = \frac{k_d}{v_{1eq} + v_{deq}} \quad (4)$$

where  $D_1$  and  $D_d$  are the diffusion coefficients of the medium and drug, respectively;  $v_1^*$  and  $v_d^*$  are the medium and drug volume fractions at interface  $R$ , respectively;  $v_{1eq}$  and  $v_{deq}$  are the medium and drug equilibrium volume fractions at rubbery-medium interface  $S$ , respectively;  $l$  is the tablet thickness; and  $k_d$  is the disentanglement rate of the polymer chains, which can be given as the ratio of the radius of gyration  $r_g$  and the reptation time  $t_{rept}$   $k_d = r_g/t_{rept}$ .

The expression for drug release (eq 2) has two different time dependencies. When the first term dominates (i.e.,  $2A \gg B^2$ ), drug release is controlled by Fickian diffusion through the gel layer, whereas Case II transport, in which drug release is controlled by polymer erosion, occurs when the second term prevails (i.e.,  $2A \ll B^2$ ). In the intermediate region, non-Fickian or anomalous transport occurs, in which drug release is a combination of both drug diffusion and polymer erosion.

## 3. EXPERIMENTAL SECTION

**3.1. Materials.** Commercial xanthan (Xan) as a yellow to tan powder with a MW of  $2 \times 10^6$  g/mol, density of 1.5 g/cm<sup>3</sup>, and viscosity of 800–1200 mPa s in 1% aqueous solution with the mean particle size of  $90 \mu\text{m} \pm 30 \mu\text{m}$  was obtained from Sigma-Aldrich Chemie, Germany. Pentoxifylline (PF), a methylxanthine derivative with MW of 278.31 g/mol, solubility in water of 77 mg/mL at 25 °C, density of 1.3 g/cm<sup>3</sup>, and mean particle size of  $60 \mu\text{m} \pm 20 \mu\text{m}$  was supplied by Krka, d.d. Novo mesto, Slovenia. For swelling and release experiments, six

media with various pH and ionic strength were used: distilled water, HCl solution at pH 3.0, and HCl at pH 1.2 according to Ph. Eur. 8th ed. and the same media with increased ionic strength  $\mu$  achieved by NaCl. The final pH values and ionic strengths of six media were: H<sub>2</sub>O ( $\mu = 0$  M), H<sub>2</sub>O ( $\mu = 0.20$  M), HCl pH 3.0 ( $\mu = 0.001$  M), HCl pH 3.0 ( $\mu = 0.20$  M), HCl pH 1.2 ( $\mu = 0.08$  M), and HCl pH 1.2 ( $\mu = 0.28$  M). The ionic strength  $\mu$  was calculated as  $\mu = 1/2 \sum_{i=1}^n c_i z_i^2$  where  $n$  is the number of all ions in the solution,  $c_i$  is the molar concentration measured in mol/L (M), and  $z_i$  is the charge number of ion  $i$ .

**3.2. Preparation of Xanthan Matrix Tablets.** Xan and the drug (PF) were mixed homogeneously using a laboratory model drum blender (Electric Inversina Tumbler Mixer, Paul Schatz principle, BioComponents Inversina 2L, Bioengineering AG, Switzerland), and three types of cylindrical flat-faced tablets with compositions (Xan, Xan:PF 3:1, and Xan:PF 1:1) were prepared by direct compression (SP 300, Kilian and Co., Cologne, Germany) to form tablets with a diameter of 12 mm and crushing strength of  $100 \text{ N} \pm 10 \text{ N}$  (Tablet hardness tester, Vanderkamp, VK 200, USA). The tablets with PF (with 100 mg or 200 mg of PF) had a mass of  $400 \text{ mg} \pm 10 \text{ mg}$  and a thickness of  $3.2 \text{ mm} \pm 0.05 \text{ mm}$ . Tablets without PF were also prepared with a mass of  $500 \text{ mg} \pm 10 \text{ mg}$  and thickness of  $4.2 \text{ mm} \pm 0.05 \text{ mm}$ . Before measurements, the moisture content of the tablets was  $7\% \pm 1\%$  determined by Büchi moisture analyzer (B-302, Büchi Labortechnik, Switzerland).

**3.3. Preparation of Gels with Known Xanthan Concentrations.** Gels with known mass ratio (w/w) Xan/medium ranging from 0.01–1.0 were prepared with H<sub>2</sub>O ( $\mu = 0$  M) and with HCl pH 1.2 ( $\mu = 0.28$  M) using three different methods. For Xan concentrations between 0.01 and 0.4, Xan was precisely weighed and dispersed in the medium with a magnetic stirrer until a uniform gel was formed. For gels at higher concentrations (from 0.4–0.6), weighed Xan powder was slightly compressed in a glass tube, and a precisely weighed amount of the medium was added. The tubes were sealed to prevent medium evaporation and left at room temperature for 2 weeks until a uniform gel was formed. The gel homogeneity was checked by 2D MR imaging, where the uniform signal intensity through the sample reveals its homogeneity. The tubes were weighed at the beginning and before the measurements to detect any medium loss during gel preparation. For higher Xan concentrations in water, tablets from Xan powder were compressed and stored in desiccators with saturated salt solutions (NaCl and NaNO<sub>2</sub>), which produce controlled relative humidity conditions. The samples were kept in the desiccators for 2 weeks to reach equilibrium water content. For the highest Xan concentration, tablets at room humidity were used.

For gels containing the model drug PF, Xan and the drug in a 1:1 ratio were mixed homogeneously using a laboratory-model drum blender and prepared in the same way as the pure Xan gels.

**3.4. NMR Relaxation Times of Xanthan Gels.** The NMR spin–lattice ( $T_1$ ) and spin–spin ( $T_2$ ) relaxation times were measured at room temperature at a <sup>1</sup>H NMR frequency  $\nu_{\text{H}} = 100$  MHz for gels of known Xan concentration in two media, water, and HCl pH 1.2 ( $\mu = 0.28$  M). The experiments were performed on a TecMag Apollo (USA) MRI spectrometer with a superconducting 2.35 T horizontal bore magnet (Oxford Instruments, UK) equipped with gradients and RF coils for MR microscopy (Bruker, Germany). The  $T_1$  time was measured by

a standard inversion recovery sequence<sup>34</sup> ( $180^\circ - \tau - 90^\circ - \text{AQ}$ ) by changing  $\tau$  values from 0.02 ms to 15 s.  $T_1$  value was determined from measurements by fitting the signal intensity ( $S$ ) obtained at different  $\tau$  values to  $S(\tau) = a_1(1 - b_1 \exp(-\tau/T_1))$ , where  $a_1$  and  $b_1$  are constants ( $b_1 \approx 2$ ). The  $T_2$  times of gels were measured using a CPMG pulse sequence<sup>35</sup> ( $90^\circ - \tau - [180^\circ - \tau - \text{AQ} - \tau]_N$ ) with  $\tau = 1$  ms and  $N = 3000$ . The  $T_2$  times of samples at high Xan concentrations for which  $T_2$  is short ( $T_2 < 5$  ms) were measured by a Hahn echo pulse sequence by changing the inter echo time from 0.02 ms to 2 s. The  $T_2$  values were determined from  $S(\tau) = a_2 + b_2 \exp(-\tau/T_2)$ , where  $a_2$  and  $b_2$  are constants.

### 3.5. MR Imaging of Xanthan Tablets during Swelling.

The tablet for MRI was inserted in a container so that only one cylinder base was exposed for the medium penetration. A tablet at room humidity, which was not in contact with the medium, was used as a reference (Figure 1). The first MR image was taken approximately 10 min after the tablet came in contact with the medium and then every 30 min for 15 h.

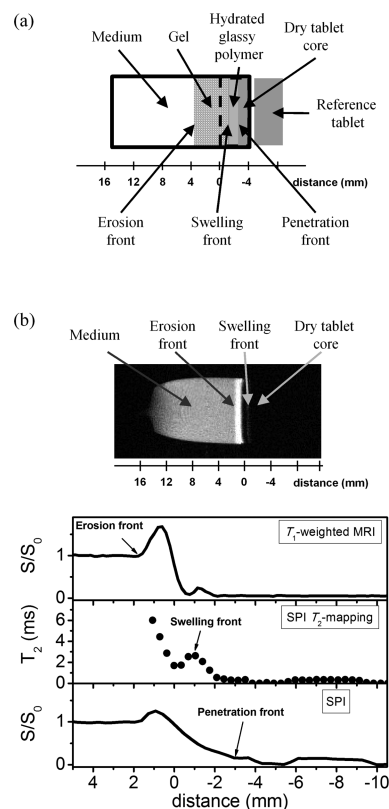


**Figure 1.** (a) Schematic presentation of the experimental setup with denoted areas and fronts forming during swelling. The dashed line indicates the position of the tablet at the beginning of the experiment. (b) 2D MR image of Xan tablet in HCl pH 1.2 ( $\mu = 0.28$  M) medium after 2.7 h of swelling with denoted areas and fronts forming during swelling as observed on  $T_1$ -weighted MR image together with determination of the moving fronts: the erosion front was obtained from one-dimensional signal intensity profile along the horizontal direction of  $T_1$ -weighted 2D MR image, the swelling front was determined from  $T_2$  profile, and the penetration front was determined from 1D SPI normalized signal intensity. The SPI signal in the region between  $-6$  mm and  $-10$  mm comes from the reference tablet that was not observed on 2D MR image due to too short  $T_2$ . Zero on  $x$  axis represents the surface of the tablet at the beginning of the experiment.

MR images were recorded at room temperature with the same spectrometer as used for the relaxation time measurements. To be able to accurately determine the penetration, swelling, and erosion front positions during tablet swelling, three different MRI methods were used (Figure 1). To measure the position of erosion front, the 2D  $T_1$ -weighted MR images were taken using a standard spin-echo pulse sequence<sup>34</sup> with an echo time ( $TE$ ) of 6.2 ms and a repetition time ( $TR$ ) of 200 ms. The field of view was 50 mm with in-plane resolution of 200  $\mu\text{m}$  and slice thickness of 3 mm. To measure the position of penetrated medium into the tablet, a one-dimensional single point imaging (1D SPI) sequence was used. A single point on the free induction decay was sampled at encoding time  $t_p = 0.17$  ms after the radiofrequency detection pulse  $\alpha = 20^\circ$  with  $TR$  of 200 ms. To measure the position of swelling front 1D  $T_2$  profiles were determined by a 1D SPI  $T_2$  mapping sequence with the same acquisition parameters as for the 1D SPI sequence was used.<sup>36</sup> The interecho time of the spin preparation CPMG echo train varied from 0.3 to 10 ms. The field of view of the SPI sequences was 45 mm with in-plane resolution of 350  $\mu\text{m}$ . The measurements were repeated at least three times for each kind of tablet and in all six media.

**3.6. Drug Release Study from Xanthan Tablets.** Two different methods were used to study drug release from Xan tablets: a standard paddle method and a “non-mixing” method that simulated conditions as used during the MRI measurements. Drug release measured by the paddle method was performed on a fully calibrated dissolution apparatus (Apparatus II, VanKel Dissolution Apparatus, model VK 7000, Cary, NC, USA). The measurement settings were the following: paddle speed 100 rpm, temperature  $37^\circ\text{C} \pm 0.5^\circ\text{C}$ , and 900 mL of medium. At predetermined time intervals, 10 mL samples were withdrawn without being replaced. The collected samples were filtered through the filter with 0.45  $\mu\text{m}$  pores, suitably diluted with the release medium, and the absorbance was measured at 274 nm (HP Agilent 8453 Diode Array UV-vis Spectrophotometer, Waldbronn, Germany).

To study drug release using the “non-mixing” method, tablets were inserted in the same containers as for MRI measurements. Medium penetration was allowed from only one circular surface, and there was no medium mixing. Ten containers with tablets were prepared for each medium. The medium (5.2 mL) was added at the same time in all the containers. At the same time points as in the paddle method, the medium was removed from one of the containers, and drug content was determined as described above. Drug release with the “non-mixing” method was measured in pure water and in HCl pH 1.2 ( $\mu = 0.28$  M) medium. At the same time, the quantity of the medium that had penetrated in the tablet at a certain time was determined as the difference between the volumes of medium added and removed and used for estimation of the dissolved PF amount.

**3.7. Statistical Analysis.** The values reported are means and standard deviations of experiments carried out at least three times. Data were analyzed using a one-way analysis of variance ( $t$ -test), and  $p < 0.05$  was considered significant.

## 4. RESULTS AND DISCUSSION

**4.1. Effect of Xanthan and Drug Loading on  $T_1$  and  $T_2$  Relaxation Times of Gels.** Starting from principles of MR, the signal intensity depends on the concentration of (usually  $^1\text{H}$ ) nuclei detected in a sample, on their relaxation times  $T_1$  and  $T_2$ , and on their self-diffusion coefficient; it is possible to accurately determine moving fronts in matrix tablets during

water penetration, swelling, and erosion.<sup>37</sup> In our study, swelling behavior of Xan tablets, empty or loaded with PF, was investigated in media differing in pH and ionic strength. First, the relaxation times of pure Xan gels and of Xan gels with 50% PF drug prepared in water and in HCl pH 1.2 ( $\mu = 0.28$  M) medium were measured at known Xan concentrations. These were the media with the largest differences in pH and ionic strengths used in the study. Monoexponential decay was observed for all  $T_1$  and  $T_2$  measurements, indicating fast exchange of water molecules between their bound and free states. Monoexponential  $T_1$  and  $T_2$  decays in gels of cellulose ethers have been observed also by other authors.<sup>8,10,13</sup> However, in gels of some other polymers, multiexponential  $T_2$  decay has been observed, and that was associated with a distribution of mesh sizes.<sup>38,39</sup> Therefore, a monoexponential  $T_2$  decay observed in Xan gels implies that the distribution of meshes of the polymeric network is narrow so that only one  $T_2$  value can be determined. However, the parameter  $a_2$  may also contain the signal of a possible long  $T_2$  component that would imply the presence of small amount of larger meshes.

At Xan concentrations below 0.8, both  $T_1$  and  $T_2$  decrease with increasing Xan concentration. The  $T_1$  relaxation time passes a minimum at Xan concentration 0.8 where the rotational correlation time  $\tau$  is of order of  $^1\text{H}$  NMR frequency  $\omega_{\text{H}}$  ( $\omega_{\text{H}}\tau \approx 1$ ). At higher concentrations,  $T_1$  increases and  $T_2$  further decreases (Figure 2). Different behavior of  $T_1$  and  $T_2$  is

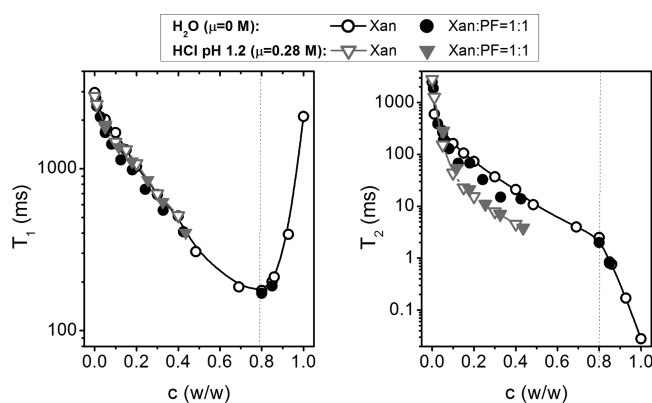


**Figure 2.** Relaxation times  $T_1$  and  $T_2$  for gels at different Xan concentrations  $c$  (w/w) prepared in  $\text{H}_2\text{O}$  ( $\mu = 0$  M) and in HCl pH 1.2 ( $\mu = 0.28$  M).

due to the fact that  $T_1$  depends on motions at  $\omega_{\text{H}}$  and  $2\omega_{\text{H}}$ , while  $T_2$  depends also on the frequency independent term<sup>34</sup> that becomes significant at  $\omega_{\text{H}}\tau \gg 1$  (i.e., at Xan concentrations higher than 0.8). Therefore,  $T_1$  probes high frequency motions, whereas  $T_2$  is sensitive to the rather slow motions. Differences in  $T_1$  relaxation times for gels formed with water and with acid medium are negligible, while  $T_2$  relaxation times for gels at pH 1.2 are significantly shorter indicating more restricted mobility of Xan chains in acid medium. The results show that the incorporated drug does not significantly change the relaxation times at any measured Xan concentration (Figure 2), meaning that MRI signal intensity depends on Xan concentration only and that the drug has negligible influence on it.

**4.2. Effect of Drug Loading on Behavior of Xanthan Tablets in Various Media.** To follow changes within the tablets during penetration, swelling, and erosion 2D spin-echo, 1D SPI, and 1D SPI  $T_2$  mapping sequences were used as described in Mikac et al.<sup>37</sup> Briefly, the border between dry and

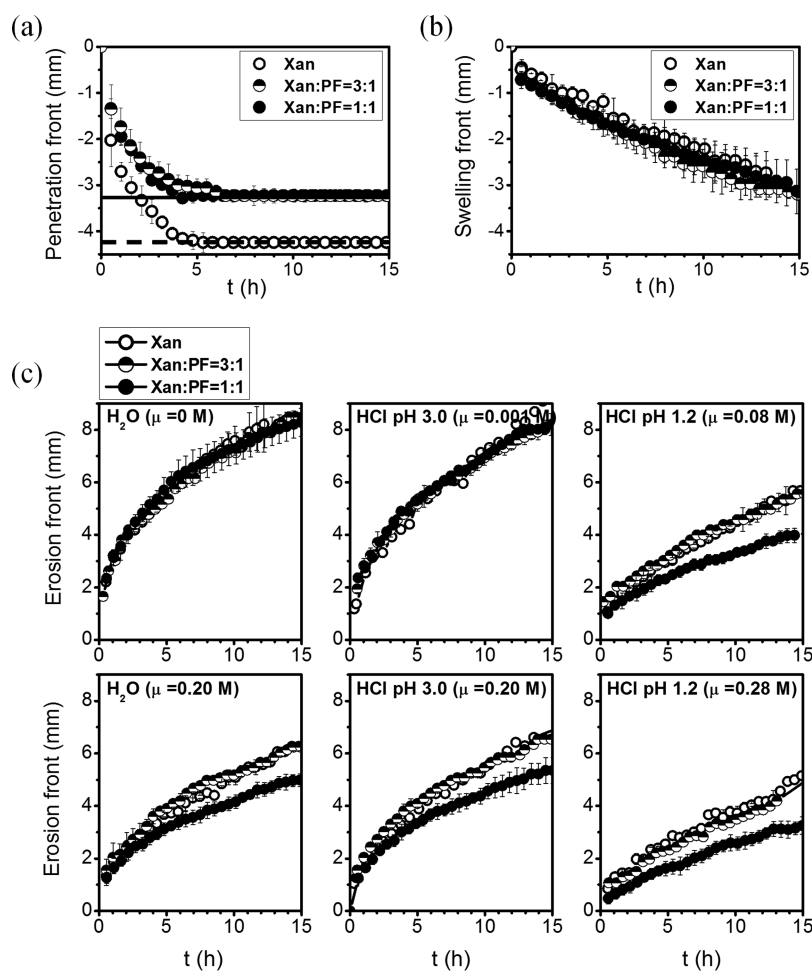


**Figure 3.** Positions of (a) penetration fronts (the solid line shows the bottom of Xan tablets loaded with PF and the dashed line shows the bottom of pure Xan tablets), (b) swelling fronts (the data of the penetration and swelling fronts represent the mean values for all six media at different values of pH and ionic strength), and (c) erosion fronts in different media for pure Xan tablets and for Xan tablets with PF at two different drug loadings. Each point represents the mean value  $\pm$  SD.

hydrated glassy Xan (the penetration front) was determined from 1D SPI signal intensity profiles. The swelling front, where Xan is transformed from a glassy to a rubbery state (gel formation), was determined from  $T_2$  profiles. The  $T_2$  value at glassy to rubbery state transition was determined to be  $2.7 \text{ ms} \pm 0.5 \text{ ms}$ . The erosion front was obtained from signal intensity profiles of  $T_1$ -weighted spin-echo MR images (Figure 1b). To imitate the physiological conditions, swelling was followed in six media, differing in pH and ionic strengths: H<sub>2</sub>O ( $\mu = 0 \text{ M}$ ), HCl pH 3.0 ( $\mu = 0.001 \text{ M}$ ), HCl pH 1.2 ( $\mu = 0.08 \text{ M}$ ), and the same media with increased ionic strengths: H<sub>2</sub>O ( $\mu = 0.20 \text{ M}$ ), HCl pH 3.0 ( $\mu = 0.20 \text{ M}$ ), and HCl pH 1.2 ( $\mu = 0.28 \text{ M}$ ).

Swelling data for pure Xan tablets and Xan tablets loaded with 25% or 50% of water-soluble PF are shown in Figure 3. The graphs represent the penetration, swelling, and erosion front positions at different times for all three types of tablets and all six media. The results showed that the media properties do not influence the position of the penetration and swelling fronts; therefore, at each swelling time, only one value (an average value across all media) for the position of the penetration front is shown in Figure 3, panel a and for the swelling front in Figure 3, panel b. The behavior of Xan matrix differs from matrix tablets with incorporated PF. The penetration front in pure Xan tablets reaches a depth of 3.2 mm (thickness of tablets with PF) in 2 h, whereas in the tablets

loaded with PF, the penetration front reaches the same depth in 4 h (Figure 3a). Irrespective of the amount of drug incorporated (25% or 50%), penetration fronts are similar. Slower medium penetration can be explained by high solubility of the PF, which uses some medium to dissolve. It is interesting that the hydration is primarily regulated by Xan despite its varying amounts in the tablets (100%, 75%, and 50%). Figure 3, panel b shows very similar swelling front kinetics for all three types of tablets in all media. The comparison of the positions of swelling and penetration fronts (Figures 3a,b) shows that the media penetrate faster, whereas the swelling is significantly slower, irrespective of whether there is an empty matrix or it is loaded with the drug. This suggests that water molecules enter the matrix quickly, but the relaxation and hydration of the polymer chains are relatively slower.

In the processes under consideration, the media properties do not influence the position of the penetration and swelling fronts but do affect the erosion front position (Figure 3c). The erosion front expansion is the fastest for the tablets in water and in HCl pH 3.0 medium and considerably slower in HCl pH 1.2. Increased ionic strength decreases the erosion front expansion in all media, although the effect is significant only in water or dilute acid medium. The situation is, however, different when the effect of drug on the swelling properties is considered. Namely, PF changes the erosion front position depending on

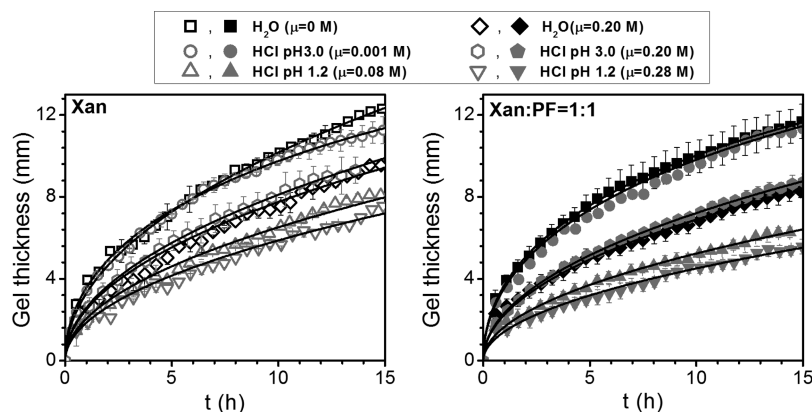


**Figure 4.** Gel layer thicknesses for pure Xan tablets (open symbols) and Xan/PF = 1:1 tablets (solid symbols) in different media. Each point represents the mean value  $\pm$  SD, and the lines are the best fits of the measured data to eq 1.

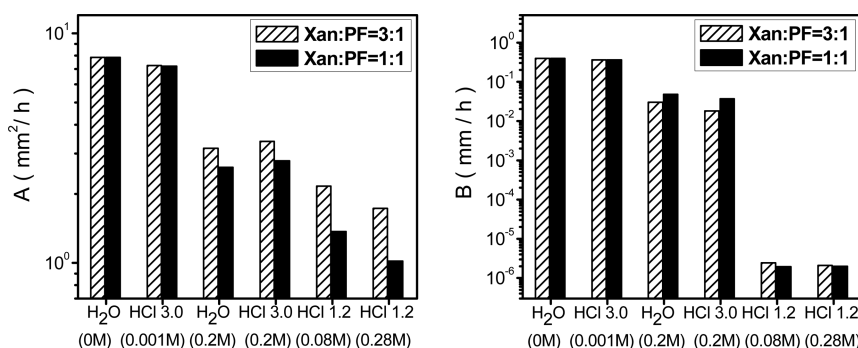


**Figure 5.** Parameters *A* and *B* obtained by fitting the time dependences of the gel layer thicknesses for various media and drug loadings to eq 1.

its amount in the tablet and on dissolution medium. The position of the erosion front is the same within experimental error for the pure Xan tablets and Xan tablets with 25% drug in all media (Figure 3c), whereas for the tablets with 50% drug, the position of the erosion front changes and is strongly influenced by media pH and high ionic strength.

The differences of the erosion front with time result in changes in the gel thickness (the distance between the erosion and swelling front positions) of Xan tablets (Figure 4). The presence of drug has no influence on the gel thickness at low (Xan/PF = 3:1) loading, whereas high drug amount (Xan/PF = 1:1) affects the thicknesses. This effect is expressed only at pH 1.2, where approximately 25% thinner gel is formed, or at increased ionic strength, whereby the gel is approximately 15% thinner than in the empty Xan tablets (Figure 4). The drug loading does not change the order of the gel thicknesses. The thickest gel is formed in water and HCl pH 3.0 ( $\mu = 0.001$  M) media, followed by a slightly thinner gel in these media with increased ionic strength, and the thinnest gel is formed in HCl pH 1.2 ( $\mu = 0.28$  M) medium.

The experimental data of gel thicknesses were compared with eq 1, and parameters *A* and *B* representing the diffusion and erosion impact, respectively, were obtained for each medium for both drug loadings (Figure 5). Both parameters decrease with increasing ionic strength or decreasing pH; however, the decrease in parameter *B* is much stronger, especially in the case of HCl pH 1.2 medium, where it decreases by five orders of magnitude compared to the *B* value obtained for water. This shows a significant decrease in the disentanglement rate  $k_d$  of the Xan chains at low pH, which is in agreement with previous measurements of the radius of gyration.<sup>40</sup> It has been shown

that the radius of gyration of xanthan's chains decreases with increased ionic strength, and an additional decrease occurs at pH 1.2. Moreover, in water and HCl pH 3.0 ( $\mu = 0.001$  M) medium, the parameters are similar for both drug loadings, whereas in other media, the parameter *A* decreases with increasing drug loading. In those media, also small differences are observed in the *B* values.

As already discussed in our previous paper,<sup>37</sup> in the presence of ions in the medium (low pH or high ionic strength), the screening effects of counterions on the negatively charged hydrophilic  $\text{COO}^-$  groups result in reduced repulsion between Xan chains. Xan chains are in an ordered state (a double-stranded helix), and the swelling is low. At higher pH or low ionic strength, ionization of acid groups is enhanced, and solubility and electrostatic repulsion between Xan chains is thus increased, leading to thicker gel layer in water and at HCl pH 3.0.

Previous studies of the impact of incorporated drug on the gel thickness of tablets made of other polymers showed different dependences. For some polymers (HPMC, low-substituted hydroxypropyl cellulose (LH41), PVP, amylose starch), the incorporation of high-soluble drug causes higher swelling, resulting in a thicker gel layer,<sup>41–43</sup> whereas in the case of low drug loading (10%) in amylose starch<sup>44</sup> and in HPMC even at high drug loading (up to 80%),<sup>7,45</sup> no significant changes in gel layer thicknesses have been observed. On the other hand, in the case of low-soluble drug with 60% loading, a thinner gel layer was observed in the HPMC matrix tablets.<sup>45</sup> It is therefore obvious that polymer swelling and the gel layer thickness are dependent not only on the percentage of drug, but also on the polymer type and drug solubility.

**4.3. Influence of Experimental Conditions on Drug Release and Release Kinetics *in Vitro*.** PF release from Xan matrix tablets was monitored in all six media (pure water, HCl pH 3, HCl pH 1.2, and the same media with increased ionic strengths) by the paddle method, whereas the “non-mixing” method was used only in pure water and in HCl pH 1.2 ( $\mu = 0.28$  M) medium, where the largest differences in polymer swelling and drug release kinetics measured with the paddle method were observed. The “non-mixing” method was introduced to simulate conditions during MR studies and to obtain more realistic correlations between formation of the gel layer and drug release.

**4.3.1. Drug Release Measured by the Paddle Method.** The drug release profiles obtained by the paddle method show a little faster release from the tablets with 50% PF compared to 25% PF only in H<sub>2</sub>O ( $\mu = 0$  M) and HCl pH 3.0 ( $\mu = 0.001$  M) medium after 5 h. In all other media, no differences were observed (Figure 6a). Comparing release profiles of the samples with the same drug loading in various media shows a completely different picture (Figure 6b). Drug release is in pure water only slightly faster than in a diluted acid medium. The releases in a high-acid medium and in media with increased ionic strength are, on the other hand, much faster. Increased ionic strength affects drug release only in water and in dilute acid medium, the effect at pH 1.2 being negligible, where the polymer is predominantly in nonionic form.

To describe the release profiles obtained using the paddle method, measured data were fitted by eq 2 with two variable parameters  $k_{\text{dif}} = \sqrt{2A} (v_{\text{deq}} + v_{\text{d}}^*)/l$  and  $k_{\text{eros}} = B (v_{\text{deq}} + v_{\text{d}}^*)/l$ . The fitting parameters obtained for each medium are shown in Figure 7. The parameter  $k_{\text{dif}}$  is zero in media with zero ionic strength and  $\text{pH} \geq 3$ , and it increases with increasing ionic strength and with decreasing pH, whereas  $k_{\text{eros}}$  slightly decreases at these conditions. The values obtained imply different release mechanisms in two cases. In water and in dilute acid medium with low ionic strength, the main release mechanism is polymer erosion, whereas in other media, anomalous transport dominates, and because  $k_{\text{dif}} \gg k_{\text{eros}}$ , the diffusion through the gel layer prevails. As expected, the release is faster in the case of diffusion-driven release than in the case of an erosion mechanism. Similar results (i.e., dependence of the release mechanism on the medium properties) have already been observed in Xan matrix tablets.<sup>46–48</sup>

Results also show that both parameters  $k_{\text{dif}}$  and  $k_{\text{eros}}$  depend on drug loading:  $k_{\text{dif}}$  decreases, whereas  $k_{\text{eros}}$  slightly increases with increasing PF amount. In pure water and HCl pH 3.0 medium, the PF release is somewhat faster from tablets with 50% PF after 5 h of swelling (Figure 6a). In this case, more diluted gel is expected on the tablet surface due to the lower amount of Xan polymer. This diluted gel is more sensitive to shear forces in the medium during drug release measurements by the paddle method, seen as faster erosion and expressed in higher  $k_{\text{eros}}$  values. The situation is different in media with increased ionic strengths, where drug release rates do not change with increasing amount of drug in the tablet (Figure 6a). Here, the erosion contribution increases as well, but the diffusion contribution decreases at higher drug loading (Figure 7).

**4.3.2. Drug Release Measured by the “Non-Mixing” Method.** Completely different results of drug loading influence on drug release were observed when measured by the “non-mixing” method in H<sub>2</sub>O ( $\mu = 0$  M) and HCl pH 1.2 ( $\mu = 0.28$  M) medium. This shows that the selection of the release

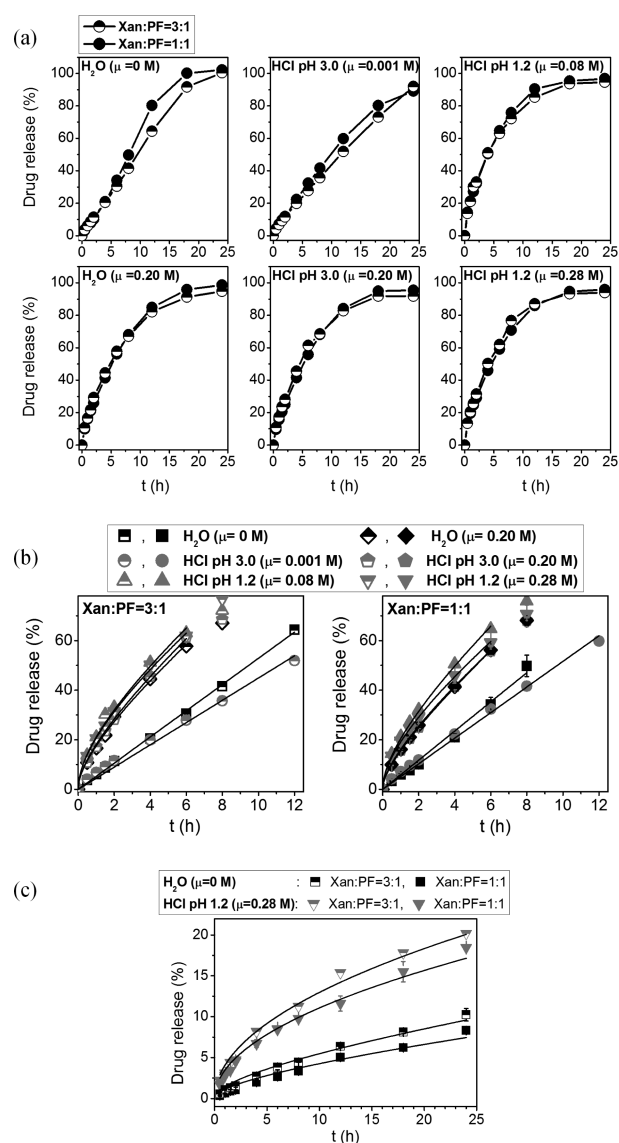


**Figure 6.** Release profiles of PF from Xan tablets in investigated media measured by the paddle method: (a) comparison between drug release from Xan/PF = 1:1 and Xan/PF = 3:1 tablets in all six media, (b) comparison of drug release profiles with the same drug loading in different media, and (c) release profiles measured by the “non-mixing” method for Xan/PF = 1:1 and Xan/PF = 3:1 tablets in H<sub>2</sub>O ( $\mu = 0$  M) and HCl pH 1.2 ( $\mu = 0.28$  M) medium. The symbols for panels b and c are measured values, and the lines are the best fits to eq 2.

experiment is of crucial importance for investigating the effect of the amount of the incorporated drug. In the case of the “non-mixing” method, faster drug release is observed for tablets containing 25% drug in both media than in tablets with 50% (Figure 6c). The effect of the media remains identical, and therefore faster release was observed in acid medium compared to water.

The influences of the media on drug release measured by the “non-mixing” method were described by fitting measured values of drug release to eq 2. For parameters  $A$  and  $B$ , the corresponding values obtained from fitting the gel layer thicknesses were used, and the fit parameter  $v_{\text{deq}} + v_{\text{d}}^*$  was determined (Table 1). The sum  $v_{\text{deq}} + v_{\text{d}}^*$  strongly depends on the medium properties; that is, it is approximately 10-times greater in acid medium than in water. The  $v_{\text{deq}} + v_{\text{d}}^*$

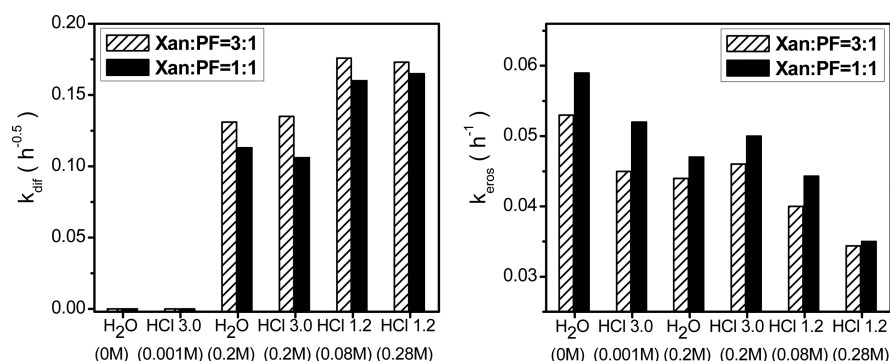


**Figure 7.** Fitting parameters  $k_{dif}$  and  $k_{eros}$ , showing the contribution of different release mechanism, determined from drug release data measured by the paddle method and fitted by eq 2.

**Table 1.** Values of Fitting Parameters  $v_{deq} + v_d^*$  Together with Calculated Values  $k_{dif}$  and  $k_{eros}$  for Two Different Drug Loadings of Xan Tablets in Water and Acid Medium for the “Non-Mixing” Method

	Xan/PF = 3:1			Xan/PF = 1:1		
	$v_{deq} + v_d^*$	$k_{dif}$ ( $1/h^{0.5}$ )	$k_{eros}$ (1/h)	$v_{deq} + v_d^*$	$k_{dif}$ ( $1/h^{0.5}$ )	$k_{eros}$ (1/h)
$H_2O$ ( $\mu = 0$ M)	0.0107	$1.3 \times 10^{-2}$	$1.3 \times 10^{-3}$	0.0083	$1 \times 10^{-2}$	$1 \times 10^{-3}$
HCl pH 1.2 ( $\mu = 0.28$ M)	0.07	$4.1 \times 10^{-2}$	$4.6 \times 10^{-8}$	0.08	$3.5 \times 10^{-2}$	$5 \times 10^{-8}$

**Table 2.** Volume of Medium Penetrated into the Tablet ( $V$ ), Amount of Maximally Dissolved PF Drug in This Medium as % of All PF in the Tablet ( $MD$ ), and Amount of Released Drug in % ( $RD$ ) for Tablets at Two Different Xan-to-PF Ratios in  $H_2O$  ( $\mu = 0$  M) and HCl 1.2 ( $\mu = 0.28$  M) Medium in “Non-Mixing” Conditions

$t$ (h)	$H_2O$ ( $\mu = 0$ M)						HCl pH 1.2 ( $\mu = 0.28$ M)					
	Xan/PF = 3:1			Xan/PF = 1:1			Xan/PF = 3:1			Xan/PF = 1:1		
	$V$ (mL)	$MD$ (%)	$RD$ (%)	$V$ (mL)	$MD$ (%)	$RD$ (%)	$V$ (mL)	$MD$ (%)	$RD$ (%)	$V$ (mL)	$MD$ (%)	$RD$ (%)
10	1.07	82	5	1.09	42	4	0.55	42	14	0.50	19	11
18	1.39	>100	8	1.31	50	7	0.66	51	20	0.67	26	17
24	1.50	>100	10	1.51	58	9	0.76	59	26	0.69	27	23

dependence on drug loading is much smaller. The reason for differences in drug volume fractions between the water and acid medium is different polymer solubility in both media and, along with that, the amount of the medium that is available for drug dissolution.

In “non-mixing” conditions, drug loading changes the drug release kinetics in the same way in water and in acid medium; that is, faster drug release is observed in Xan tablets with 25% drug in both media. However, the reason for faster drug release at lower drug loading is different. In water, the sum  $v_{deq} + v_d^*$  is higher at lower drug loading, indicating a higher amount of dissolved drug that can be released from the tablet, and because parameters  $A$  and  $B$  are the same for both drug loadings (Figure 5), a different amount of dissolved drug is the reason for different drug release kinetics in water under still conditions. In an acid medium, the sum  $v_{deq} + v_d^*$  is lower at lower drug loading, which would imply slower drug release (Table 1). However, parameter  $A$  is larger for 25% drug loading, and the value of parameter  $B$  is the same for both drug loadings (Figure 5), which results in faster drug release at lower drug loading despite the thicker gel layer (Figures 4 and 6c). Therefore, in the acid medium, the gel structure that enables faster drug diffusion through the gel layer is the reason for faster drug release at lower drug loading.

From the model parameters  $A$ ,  $B$ , and  $v_{deq} + v_d^*$ , the parameters  $k_{dif}$  and  $k_{eros}$  were calculated (Table 1) and compared to drug release results measured by the paddle method (Figure 7). In the case of the “non-mixing” method, the

parameters  $k_{dif}$  and  $k_{eros}$  are much smaller than in the case of the paddle method, showing much slower drug release under still conditions.

There are two reasons for slower drug release measured by the “non-mixing” method in comparison with drug release measured by the paddle method. The first reason is that in the case of the paddle method in contrast to the “non-mixing” method, the medium is stirred, which increases the gel erosion. This is expressed in water, where the value of diffusion parameter  $k_{dif}$  increases compared to the  $k_{dif}$  value obtained with the paddle method. The increase in the diffusion contribution shows that drug diffusion through the gel layer also contributes to drug release under still conditions owing to smaller tablet erosion. In the case of HCl pH 1.2 ( $\mu = 0.28$  M) medium, the diffusion contribution prevails for both methods, which indicates a much lower effect of erosion even in the case of mixing. This implies the formation of more rigid gel in an acid medium, which is in agreement with shorter  $T_2$  values measured in gels prepared with acid medium than in water at the same Xan concentrations and prevailing diffusion-regulated drug release.

The second reason for the slower drug release in the “non-mixing” conditions is that the containers used for the “non-mixing” and for the paddle methods are not the same. In the “non-mixing” conditions, the amount of medium is much smaller, and the medium can penetrate into the tablet from only one circular surface, whereas in the case of the paddle method, the medium can penetrate into the tablet from all



tablet surfaces, and the amount of medium in the container is much larger. Therefore, at the same swelling time, a higher amount of the medium is in the tablet when the paddle method is applied, and consequently more medium is available for polymer swelling as well as for drug dissolution. To check this, the quantity of the medium that has penetrated into the tablet was measured at different swelling times for the “non-mixing” method.

The results of the measured volume of penetrated medium in the tablet ( $V$ ), the maximum possible quantity of dissolved PF in this medium ( $MD$ ), and the measured amount of released PF from the Xan tablet by the “non-mixing” method ( $RD$ ) are listed in Table 2. Data are shown for later times when the medium had already hydrated the entire tablet. From the data, it can be seen that, especially in the case of an acid medium, the amount of medium in the tablet is too low to dissolve the total amount of the present PF. It is even more evident in the case of higher drug loading. In water, the amount of the maximally dissolved drug in the tablet ( $MD$ ) is much higher, but it should be stressed that Xan is also highly soluble in water,<sup>49,50</sup> and it is therefore expected that Xan will use a notable amount of the medium. Thus, in reality, a lower amount of water is available for drug dissolution. This is indeed the case because in water lower values of drug volume fractions  $\nu_{\text{deq}} + \nu_{\text{d}}^*$  were determined than in acid medium (Table 1), indicating that in a realistic case even less medium is available for drug dissolution in water than in an acid medium. This shows that the amount of medium in the tablet (and, with this, drug dissolution) is the limiting process for drug release under still conditions.

**4.4. Correlation between Gel Thickness and Drug Release.** The lack of correlation between drug release and gel thickness shows that not only simple gel thicknesses, but also the gel structure is the most important factor for drug release kinetics from Xan matrix tablets. Namely, the gel structure is expected to be different under different environment conditions. In media with high pH and low ionic strength, Xan chains repel each other due to the anionic nature of Xan polymer, and polymer chains are highly hydrated. Hydrophilic groups are exposed to interaction with water, which results in rapid and extensive swelling. Consequently, abundant homogeneous gel with relatively small pores is formed. Xan is an acidic polymer<sup>44</sup> with a  $pK_a$  of 3.1 and is therefore less soluble at pH 1.2, where its carboxylic groups are mostly unionized. In the presence of ions in the medium, they screen the primary Xan charges, resulting in reduced repulsion between Xan chains. Xan chains are in an ordered state (a double-stranded helix), and the swelling is low. This results in large regions of low microviscosity and increase the total porosity of the gel.<sup>40,47,51,52</sup> On the basis of our results, the polymeric meshes are large enough to allow efficient PF diffusion through the gel layer, and in these media, drug release is mainly governed by drug diffusion through the layer. Drug diffusion is even faster at lower drug loading (higher  $k_{\text{dif}}$  values with regard to 50% drug loading for both methods measured; Figure 7 and Table 1), where, owing to a higher amount of Xan in the tablet, larger areas of poorly hydrated cores may be present in the matrix, and consequently larger meshes are expected. Similar results were also observed for hydrophobically modified poly(acrylic acid) (HMPAA). In pure HMPAA, a nonhomogeneous region containing partially swollen particles has been observed (such as Xan in pH 1.2), whereas homogeneous gel has been formed

in the case of HMPAA neutralized with NaOH (such as Xan in water).<sup>20</sup>

The results presented in this paper support our recently published work in which we established that the medium's pH and ionic strength affect the swelling dynamics and gel formation of Xan matrix tablets and consequently influence the drug release kinetics.<sup>37</sup> This finding was later confirmed by subtle AFM measurements of crude Xan powder in the same media and calculation of single polymer chain parameters, such as end-to-end distance, contour length, radius of gyration, and persistence length of individual Xan molecules.<sup>40</sup>

The results of Xan swelling and PF release kinetics in the “non-mixing” conditions were in good agreement with the pseudosteady approximation of the mathematical model that accounts for the superposition of Fickian diffusion and polymer erosion processes. The obtained model parameters show that in water the diffusion contribution to drug release is smaller than in the acid medium due to smaller value of the sum  $\nu_{\text{deq}} + \nu_{\text{d}}^*$  indicating lower fraction of dissolved drug. The erosion contribution is, on the other hand, higher in water due to higher  $B$  value. In the acid medium, the diffusion contribution leads to faster drug release, and owing to much lower  $B$  value and with that lower disentanglement rate of Xan polymer chains, to the thinner gel. The obtained parameters also show that at higher drug amount in Xan tablets drug release is slower due to lower values of  $\nu_{\text{deq}} + \nu_{\text{d}}^*$  in water and in the case of acid medium due to lower value of the parameter  $A$ , that is, slower diffusion.

The mathematical model thus shows that the additional limiting factor for drug release kinetics is drug dissolution in available medium within the matrix. This was proven in the case of release in the “non-mixing” conditions, where the amount of the medium in the tablet was too low to dissolve the total amount of drug in the tablet even at times when the entire tablet was already perfused with the medium. The same can also be present in the case of drug release measured by the paddle method, where the entire tablet is exposed to medium penetration, and a higher amount of medium is expected to be in the tablet. Nevertheless, the amount of medium in the hydrated part of the tablet can, especially at shorter times, be too small to enable dissolution of the entire quantity of drug, which can additionally retard the drug release. Therefore, in addition to the gel thickness and its structure, the amount of the medium in the tablet that is available for drug dissolution also seems to be a limiting factor for PF release from Xan tablets. This should be considered for a more realistic design of the tablets.

## 5. CONCLUSIONS

In the present study, we focused on Xan matrix tablets loaded with highly soluble PF to explore the relationship between the Xan swelling and PF release in the media with gastric pH and ionic strength. The results based on MR imaging, drug release measurements, and mathematical analysis indicated decisive influence of Xan and significantly smaller impact of PF also at the high ratios Xan/PF 3:1 or 1:1. Water penetrates in empty Xan faster than in Xan with PF, swelling is in both cases similar, and erosion front expansion drastically decreases in the tablets with 50% PF at high ionic strength and pH 1.2. The release profiles in various media were measured and matched with the predictions of a mathematical model, which combines the polymer swelling kinetics and drug diffusion to obtain release mechanism. In water and in diluted acid medium with low ionic

strength, the main release mechanism is erosion, whereas in other media (pH 1.2,  $\mu \geq 0.20$  M), anomalous transport dominates owing to changes in polymer structure. As expected, the release is faster in the case of diffusion-driven release than in the case of an erosion mechanism. Drug release measured by the paddle method is the same for different drug loadings in media with low pH or high ionic strength, whereas faster drug release is observed for higher drug loading in water or diluted acid medium that is attributed to weaker gel, which is more susceptible to erosion. By comparing drug release measured by the paddle and by the “non-mixing” method, it was shown that, in addition to the gel thickness and its structure, the amount of the medium in the tablet that is available for PF dissolution is also a limiting factor for drug release.

Polyelectrolytes are much more complicated than non-electrolyte polymeric systems due to the increased sensitivity on pH value, ionic strength, and stirring speed of the medium. Therefore, the specific properties of the Xan at the certain place make it a fascinating niche for drug delivery development.

## AUTHOR INFORMATION

### Corresponding Author

\*E-mail: [urska.mikac@ijs.si](mailto:urska.mikac@ijs.si). Phone: +386 1 477 3314. Fax: +386 1 477 3191.

### Author Contributions

This manuscript was written through contributions by all of the authors. All of the authors have given their approval to the final version of the manuscript.

### Notes

The authors declare no competing financial interest.

## ACKNOWLEDGMENTS

The authors gratefully acknowledge the Ministry of Education, Science, and Sport of the Republic of Slovenia and the Slovenian Research Agency for financial support through the research programs P1-0189 and P1-0060 and project J1- 6746.

## ABBREVIATIONS

MR, magnetic resonance; MRI, magnetic resonance imaging; NMR, nuclear magnetic resonance; PF, pentoxifylline; Xan, xanthan

## REFERENCES

- (1) Colombo, P.; Santi, P.; Bettini, R.; Brazel, S. B.; Peppas, N. A. Drug release from swelling controlled systems. In *Handbook of Pharmaceutical Controlled Release Technology*; Wise, D. L., Ed.; Marcel Dekker: New York, 2000; pp 183–209.
- (2) Ferrero Rodrigues, C.; Bruneau, N.; Barra, J.; Alfonso, D.; Doelker, E. Hydrophilic cellulose derivatives as drug delivery carriers: The influence of substitution type on the properties of compressed matrix tablets. In *Handbook of Pharmaceutical Controlled Release Technology*; Wise, D. L., Ed.; Marcel Dekker: New York, 2000; pp 1–30.
- (3) Schiller, C.; Frohlich, C. P.; Giessmann, T.; Siegmund, W.; Monnikes, H.; Hosten, N.; Weitschies, W. Intestinal fluid volumes and transit of dosage forms as assessed by magnetic resonance imaging. *Aliment. Pharmacol. Ther.* **2005**, *22*, 971–979.
- (4) Sjogren, E.; Abrahamsson, B.; Augustijns, P.; Becker, D.; et al. In vivo methods for drug absorption - Comparative physiologies, model selection, correlations with in vitro methods (IVIVC), and applications for formulation/API/excipient characterization including food effects. *Eur. J. Pharm. Sci.* **2014**, *57*, 99–151.
- (5) Koziolok, M.; Garbacz, G.; Neumann, M.; Weitschies, W. Simulating the Postprandial Stomach: Biorelevant Test Methods for

the Estimation of Intragastic Drug Dissolution. *Mol. Pharmaceutics* **2013**, *10*, 2211–2221.

- (6) Cascone, S.; De Santis, F.; Lamberti, G.; Titomanlio, G. The influence of dissolution conditions on the drug ADME phenomena. *Eur. J. Pharm. Biopharm.* **2011**, *79*, 382–391.

- (7) Colombo, P.; Bettini, R.; Peppas, N. A. Observation of swelling process and diffusion front position during swelling in hydroxypropyl methylcellulose (HPMC) matrices containing a soluble drug. *J. Controlled Release* **1999**, *61*, 83–91.

- (8) Baumgartner, S.; Lahajnar, G.; Sepe, A.; Kristl, J. Investigation of the state and dynamics of water in hydrogels of cellulose ethers by 1H NMR spectroscopy. *AAPS PharmSciTech* **2002**, *3*, 86.

- (9) Baumgartner, S.; Lahajnar, G.; Sepe, A.; Kristl, J. Quantitative evaluation of polymer concentration profile during swelling of hydrophilic matrix tablets using 1H NMR and MRI methods. *Eur. J. Pharm. Biopharm.* **2005**, *59*, 299–306.

- (10) Chen, Y. Y.; Hughes, L. P.; Gladden, L. F.; Mantle, M. D. Quantitative ultra-fast MRI of HPMC swelling and dissolution. *J. Pharm. Sci.* **2010**, *99*, 3462–3472.

- (11) Nott, K. P. Magnetic resonance imaging of tablet dissolution. *Eur. J. Pharm. Biopharm.* **2010**, *74*, 78–83.

- (12) Mikac, U.; Kristl, J.; Baumgartner, S. Using quantitative magnetic resonance methods to understand better the gel-layer formation on polymer-matrix tablets. *Expert Opin. Drug Delivery* **2011**, *8*, 677–692.

- (13) Kulinowski, P.; Mlynarczyk, A.; Dorozynski, P.; Jasinski, K.; Gruwel, M. L. H.; Tomanek, B.; Weglarz, W. P. Magnetic resonance microscopy for assessment of morphological changes in hydrating hydroxypropylmethyl cellulose matrix tablets in situ. *Pharm. Res.* **2012**, *29*, 3420–3433.

- (14) Barba, A. A.; D'Amore, M.; Cascone, S.; Chirico, S.; Lamberti, G.; Titomanlio, G. On the behavior of HPMC/theophylline matrices for controlled drug delivery. *J. Pharm. Sci.* **2009**, *98*, 4100–4110.

- (15) Jamzad, S.; Tutunji, L.; Fassihi, R. Analysis of macromolecular changes and drug release from hydrophilic matrix systems. *Int. J. Pharm.* **2005**, *292*, 75–85.

- (16) Lamberti, G.; Cascone, S.; Cafaro, M.; Titomanlio, G.; d'Amore, M.; Barba, A. A. Measurements of water content in hydroxypropylmethyl-cellulose based hydrogels via texture analysis. *Carbohydr. Polym.* **2013**, *92*, 765–768.

- (17) Fyfe, C. A.; Grondey, H.; Blazek-Welsh, A. I.; Chopra, S. K.; Fahie, B. J. NMR imaging investigations of drug delivery devices using a flow-through USP dissolution apparatus. *J. Controlled Release* **2000**, *68*, 73–83.

- (18) Shiko, G.; Gladden, L. F.; Sederman, A. J.; Connolly, P. C.; Butler, J. M. MRI studies of the hydrodynamics in a USP 4 dissolution testing cell. *J. Pharm. Sci.* **2011**, *100*, 976–991.

- (19) Banerjee, A.; Chandrakumar, N. Real-time in vitro drug dissolution studies of tablet using volume-localized NMR (MRS). *Appl. Magn. Reson.* **2011**, *40*, 251–259.

- (20) Knoos, P.; Topgaard, D.; Wahlgren, M.; Ulvenlund, S.; Piculell, L. Using NMR chemical shift imaging to monitor swelling and molecular transport in drug-loaded tablets of hydrophobically modified poly(acrylic acid): methodology and effects of polymer (in)solubility. *Langmuir* **2013**, *29*, 13898–13908.

- (21) Fyfe, C. A.; Blazek, A. I. Investigation of hydrogel formation from hydroxypropylmethylcellulose (HPMC) by NMR spectroscopy and NMR imaging techniques. *Macromolecules* **1997**, *30*, 6230–6237.

- (22) Dahlberg, C.; Dvinskikh, S. V.; Schuleit, M.; Furo, I. Polymer swelling, drug mobilization and drug recrystallization in hydrating solid dispersion tablets studied by multinuclear NMR microimaging and spectroscopy. *Mol. Pharmaceutics* **2011**, *8*, 1247–1256.

- (23) Zhang, Q.; Gladden, L.; Avalle, P.; Mantle, M. In vitro quantitative 1H and 19F nuclear magnetic resonance spectroscopy and imaging studies of fluvastatin<sup>TM</sup> in Lescol<sup>®</sup> XL tablets in a USP-IV dissolution cell. *J. Controlled Release* **2011**, *156*, 345–354.

- (24) Caccavo, D.; Cascone, S.; Lamberti, G.; Barba, A. A. Modeling the Drug Release from Hydrogel-Based Matrices. *Mol. Pharmaceutics* **2015**, *12*, 474–483.

- (25) Garcia-Ochoa, F.; Santos, V. E.; Casas, J. A.; Gomez, E. Xanthan gum: production, recovery, and properties. *Biotechnol. Adv.* **2000**, *18*, 549–579.
- (26) Capron, I.; Brigand, G.; Muller, G. About the native and renatured conformation of xanthan exopolysaccharide. *Polymer* **1997**, *38*, S289–S295.
- (27) Chazeau, L.; Milas, M.; Rinaudo, M. Conformations of xanthan in solution analysis by steric exclusion chromatography. *Int. J. Polym. Anal. Charact.* **1995**, *2*, 21–29.
- (28) Kostewicz, E. S.; Abrahamsson, B.; Brewster, M.; Brouwers, J.; Butler, J.; Carler, S.; Dickinson, P. A.; Dressman, J.; Holm, R.; Klein, S.; et al. More In vitro models for the prediction of in vivo performance of oral dosage forms. *Eur. J. Pharm. Sci.* **2014**, *57*, 342–366.
- (29) Siepman, J.; Siepman, F. Mathematical modeling of drug delivery. *Int. J. Pharm.* **2008**, *364*, 328–343.
- (30) Kaunisto, E.; Abrahmsen-Alami, S.; Borgquist, P.; Larsson, A.; Nilsson, B.; Axelsson, A. A mechanistic modelling approach to polymer dissolution using magnetic resonance microimaging. *J. Controlled Release* **2010**, *147*, 232–241.
- (31) Lamberti, G.; Galdi, I.; Barba, A. A. Controlled release from hydrogel-based solid matrices. A model accounting for water up-take, swelling and erosion. *Int. J. Pharm.* **2011**, *407*, 78–86.
- (32) Caccavo, D.; Cascone, S.; Lamberti, G.; Barba, A. A. Controlled drug release from hydrogel-based matrices: Experiments and modeling. *Int. J. Pharm.* **2015**, *486*, 144–152.
- (33) Narasimhan, B.; Peppas, N. A. Molecular analysis of drug delivery systems controlled by dissolution of the polymer carrier. *J. Pharm. Sci.* **1997**, *86*, 297–304.
- (34) Callaghan, P. T. *Principles of Nuclear Magnetic Resonance Microscopy*; Oxford University Press Inc.: New York, 1991.
- (35) Meiboom, S.; Gill, D. Modified spin-echo method for measuring nuclear relaxation times. *Rev. Sci. Instrum.* **1958**, *29*, 688–691.
- (36) Beyea, S. D.; Balcom, B. J.; Prado, P. J.; Cross, A. R.; Kennedy, C. B.; Armstrong, R. L.; Bremner, T. W. Relaxation time mapping of short T2\* nuclei with single-point imaging (SPI) methods. *J. Magn. Reson.* **1998**, *135*, 156–164.
- (37) Mikac, U.; Sepe, A.; Kristl, J.; Baumgartner, S. A new approach combining different MRI methods to provide detailed view on swelling dynamics of xanthan tablets influencing drug release at different pH and ionic strength. *J. Controlled Release* **2010**, *145*, 247–256.
- (38) Turco, G.; Donati, I.; Grassi, M.; Marchioli, G.; Lapasin, R.; Paoletti, S. Mechanical spectroscopy and relaxometry on alginate hydrogels: A comparative analysis for structural characterization and network mesh size determination. *Biomacromolecules* **2011**, *12*, 1272–1282.
- (39) Halib, N.; Mohd Amin, M. C. I.; Ahmad, I.; Abrami, M.; Fiorentino, S.; Farra, R.; Grassi, G.; Musiani, F.; Lapasin, R.; Grassi, M. Topological characterization of a bacterial cellulose–acrylic acid polymeric matrix. *Eur. J. Pharm. Sci.* **2014**, *62*, 326–333.
- (40) Govedarica, B.; Sovany, T.; Pintye-Hodi, K.; Škarabot, M.; Baumgartner, S.; Mušević, I.; Srčić, S. Addressing potent single molecule AFM study in prediction of swelling and dissolution rate in polymer matrix tablets. *Eur. J. Pharm. Biopharm.* **2012**, *80*, 217–225.
- (41) Kojima, M.; Nakagami, H. Investigation of water mobility and diffusivity in hydrating micronized low-substituted hydroxypropyl cellulose, hydroxypropylmethyl cellulose, and hydroxypropyl cellulose matrix tablets by magnetic resonance imaging (MRI). *Chem. Pharm. Bull.* **2002**, *50*, 1621–1624.
- (42) Wang, Y. J.; Ravenelle, F.; Zhu, X. X. NMR imaging study of cross-linked high-amylose starch tablets – The effect of drug loading. *Can. J. Chem.* **2010**, *88*, 202–207.
- (43) Kowalczyk, J.; Tritt-Goc, J. A possible application of magnetic resonance imaging for pharmaceutical research. *Eur. J. Pharm. Sci.* **2011**, *42*, 354–364.
- (44) Therien-Aubin, H.; Zhu, X. X.; Ravenelle, F.; Marchessault, R. H. Membrane formation and drug loading effects in high amylose starch tablets studied by NMR imaging. *Biomacromolecules* **2008**, *9*, 1248–1254.
- (45) Tajarobi, F.; Abrahmsen-Alami, S.; Carlsson, A. S.; Larsson, A. Simultaneous probing of swelling, erosion and dissolution by NMR-microimaging – Effect of solubility of additives on HPMC matrix tablets. *Eur. J. Pharm. Sci.* **2009**, *37*, 89–97.
- (46) Talukdar, M. M.; Kinget, R. Swelling and drug release behaviour of xanthan gum matrix tablets. *Int. J. Pharm.* **1995**, *120*, 63–72.
- (47) Mu, X.; Tobby, M. J.; Staniforth, J. N. Influence of physiological variables on the in vitro drug-release behavior of a polysaccharide matrix controlled-release system. *Drug Dev. Ind. Pharm.* **2003**, *29*, 19–29.
- (48) Baumgartner, S.; Pavli, M.; Kristl, J. Effect of calcium ions on the gelling and drug release characteristics of xanthan matrix tablets. *Eur. J. Pharm. Biopharm.* **2008**, *69*, 698–707.
- (49) Talukdar, M. M.; Michael, A.; Rombaut, P.; Kinget, R. Comparative study on xanthan gum and hydroxypropylmethyl cellulose as matrices for controlled-release drug delivery I. Compaction and in vitro drug release behaviour. *Int. J. Pharm.* **1996**, *129*, 233–241.
- (50) Rinaudo, M. Relation between the molecular structure of some polysaccharides and original properties in sol and gel states. *Food Hydrocolloids* **2001**, *15*, 433–400.
- (51) Sorbie, K. S.; Huang, Y. The effect of pH on the flow behavior of xanthan solution through porous media. *J. Colloid Interface Sci.* **1992**, *149*, 303–313.
- (52) Bueno, V. B.; Bentini, R.; Catalani, L. H.; Petri, D. F. S. Synthesis and swelling behavior of xanthan-based hydrogels. *Carbohydr. Polym.* **2013**, *92*, 1091–1099.